

# Acoustic Scattering Problems with Convolution Quadrature and the Method of Fundamental Solutions

I. Labarca and R. Hiptmair

Research Report No. 2020-49  
July 2020

Seminar für Angewandte Mathematik  
Eidgenössische Technische Hochschule  
CH-8092 Zürich  
Switzerland

# ACOUSTIC SCATTERING PROBLEMS WITH CONVOLUTION QUADRATURE AND THE METHOD OF FUNDAMENTAL SOLUTIONS\*

IGNACIO LABARCA<sup>†</sup> AND RALF HIPTMAIR<sup>‡</sup>

**Abstract.** Time domain acoustic scattering problems in two and three dimensions are studied. The numerical scheme consists in the use of Convolution Quadrature method to reduce the time domain problem to solve frequency domain Helmholtz equations with complex wavenumbers. These equations are solved with the method of fundamental solutions (MFS), which approximates the solution by a linear combination of fundamental solutions defined at source points inside (outside) the scatterer for exterior (interior) problems. Numerical results show that the coupling of both methods works efficiently and accurately for multistep and multistage based CQ.

**Key words.** acoustic wave scattering, convolution quadrature, method of fundamental solutions

**1. Introduction.** Wave propagation problems have been widely studied in the time domain during last years. Much this attention is directed to the convolution quadrature (CQ) method presented by Lubich [13, 14], which uses information in the Laplace domain to solve problems in time domain. This approach was successful in the wave propagation context, because it allows the use of frequency-domain Green function instead of time-domain. Then it is possible to use integral equation methods to solve the arising frequency-domain problems. Integral equation methods are also an option in time-domain, but requires difficult integration techniques in two dimensions, and dealing with distributional expressions in three dimensions [10]. Instead of resorting to integral equations, we follow a different and simpler approach. This is the method of fundamental solutions (MFS) [7, 3] which assumes that the solution of the Helmholtz equation can be represented by a linear combination of fundamental solutions with sources located at the interior of the scatterer. The advantage of MFS for the CQ scheme also lays in the possibility of sparsification of the resulting matrix, due to the exponential decaying of fundamental solutions for modified Helmholtz equations [6]. It is also possible to use techniques developed for Boundary Element methods, which allow the use of directional  $\mathcal{H}$ -matrices for each of the Helmholtz problems [5]. Although a combination of MFS with Laplace transform techniques and the modified Helmholtz equation has been mentioned before [6, 12], as far as we know, there are no results for a successful implementation of MFS in combination of multistep and multistage methods in time domain, in which CQ is based.

The problem that we are interested in solving is the exterior acoustic scattering problem in the time-domain. Let  $\Omega \subset \mathbb{R}^d$ ,  $d = 2, 3$ , the bounded region of space occupied by the scatterer. By rescaling we can achieve that the wave speed in  $\mathbb{R}^d \setminus \bar{\Omega}$  is given by  $c = 1$ . The equations for the scattered field  $u$  are as follows [16, Section 1.5]

$$(1.1) \quad \begin{cases} \frac{\partial^2 u}{\partial t^2}(\mathbf{x}, t) - \Delta u(\mathbf{x}, t) = 0, & \mathbf{x} \in \mathbb{R}^d \setminus \bar{\Omega}, \quad t \geq 0, \\ u(\mathbf{x}, t) = -u^{\text{inc}}(\mathbf{x}, t), & \mathbf{x} \in \Gamma := \partial\Omega, \quad t \geq 0, \\ u(\mathbf{x}, 0) = \frac{\partial u}{\partial t}(\mathbf{x}, 0) = 0, & \mathbf{x} \in \mathbb{R}^d \setminus \Omega. \end{cases}$$

---

\*Date: July 13, 2020

**Funding:** This work was funded by SNF Grant 200021\_184848/1 “Novel BEM for Electromagnetics”

<sup>†</sup>Seminar for Applied Mathematics, ETH Zürich, Zürich, Switzerland ([ignacio.labarca@sam.math.ethz.ch](mailto:ignacio.labarca@sam.math.ethz.ch)).

<sup>‡</sup>Seminar for Applied Mathematics, ETH Zürich, Zürich, Switzerland ([ralf.hiptmair@sam.math.ethz.ch](mailto:ralf.hiptmair@sam.math.ethz.ch)).

This is a wave equation with Dirichlet boundary conditions and zero initial conditions. At an initial time  $t = 0$  it is assumed that the incident field has not yet reached the scatterer, which is reflected by our initial conditions.

Fundamental solutions for the wave equation in two and three dimensions centered at a given point  $\mathbf{y} \in \Omega$  are the following

$$(1.2) \quad \mathcal{G}(\mathbf{x} - \mathbf{y}, t) = \begin{cases} \frac{H(t - |\mathbf{x} - \mathbf{y}|)}{2\pi\sqrt{t^2 - |\mathbf{x} - \mathbf{y}|^2}}, & d = 2, \\ \frac{\delta(t - |\mathbf{x} - \mathbf{y}|)}{4\pi|\mathbf{x} - \mathbf{y}|}, & d = 3. \end{cases}$$

This problem has been efficiently solved in [2] by means of the convolution quadrature method and the boundary element method. We propose an alternative method based on convolution quadrature combined with the method of fundamental solutions, which is easy to implement and produces accurate numerical results.

## 2. Numerical Scheme.

**2.1. Convolution Quadrature.** We proceed to give the approach from the initial boundary value problem. We start with the wave equation, boundary conditions and initial conditions and derive frequency-domain problems based on multistep and multistage methods. Further details can be found in [10, Chapters 3, 4 and 6] and [16, Section 4].

We start by rewriting (1.1) as a first-order system in time. Let  $v(\mathbf{x}, t) := \frac{\partial u}{\partial t}(\mathbf{x}, t)$  and define

$$(2.1) \quad U(\mathbf{x}, t) := (u(\mathbf{x}, t), v(\mathbf{x}, t)).$$

From (1.1) it is clear that  $U$  satisfies

$$(2.2) \quad \begin{aligned} \frac{\partial U}{\partial t}(\mathbf{x}, t) &= \mathcal{L}U(\mathbf{x}, t), & \mathbf{x} \in \mathbb{R}^d \setminus \bar{\Omega}, \quad t \geq 0, \\ U(\mathbf{x}, t) &= -U^{\text{inc}}(\mathbf{x}, t), & \mathbf{x} \in \Gamma := \partial\Omega, \quad t \geq 0, \\ U(\mathbf{x}, 0) &= \mathbf{0}, & \mathbf{x} \in \mathbb{R}^d \setminus \bar{\Omega}, \end{aligned}$$

where  $\mathcal{L} := \begin{pmatrix} 0 & I \\ \Delta & 0 \end{pmatrix}$  and  $U^{\text{inc}}(\mathbf{x}, t) := \begin{pmatrix} u^{\text{inc}}(\mathbf{x}, t), \\ \frac{\partial u^{\text{inc}}}{\partial t}(\mathbf{x}, t) \end{pmatrix}$ .

The system (2.2) can be discretized in time by multistep or multistage methods. Finding equations in the Laplace domain will lead to the corresponding CQ scheme and will be explained in the following sections.

**2.2. Multistep Convolution Quadrature.** A multistep method for solving equation (2.2) is defined by parameters  $\alpha_\ell, \beta_\ell \in \mathbb{R}$ ,  $\ell = 0, \dots, m$  and a time step  $\Delta t > 0$  with discrete times  $t_n = n\Delta t$  such that the new unknown corresponds to  $U_n(\mathbf{x}) \approx U(\mathbf{x}, t_n)$ ,  $n = 0, 1, \dots$  in

$$(2.3) \quad \sum_{\ell=0}^m \alpha_{\ell} U_{n+\ell-m} = \Delta t \sum_{\ell=0}^m \beta_{\ell} \mathcal{L}U_{n+\ell-m}, \quad n = 0, 1, \dots$$

The use of the Z-Transform

$$(2.4) \quad \mathbf{U}(\mathbf{x}, \zeta) := \sum_{n=0}^{\infty} U_n(\mathbf{x}) \zeta^n = \sum_{n=0}^{\infty} (u_n(\mathbf{x}), v_n(\mathbf{x})) \zeta^n, \quad \zeta \in \mathbb{C}, |\zeta| < 1,$$

on (2.3) leads to a new equation in the Z-domain that corresponds to

$$(2.5) \quad \frac{\delta(\zeta)}{\Delta t} \mathbf{U}(\mathbf{x}, \zeta) = \mathcal{L}\mathbf{U}(\mathbf{x}, \zeta),$$

where  $\delta(\zeta) = \frac{\sum_{\ell=0}^m \alpha_{m-\ell} \zeta^{\ell}}{\sum_{\ell=0}^m \beta_{m-\ell} \zeta^{\ell}}$ . We also obtain valid boundary conditions in the Z-domain,

$$(2.6) \quad \mathbf{U}(\mathbf{x}, \zeta) = -\mathbf{U}^{\text{inc}}(\mathbf{x}, \zeta) := -\sum_{n=0}^{\infty} U^{\text{inc}}(\mathbf{x}, t_n) \zeta^n, \quad \mathbf{x} \in \Gamma.$$

Finally, we obtain the following boundary value problem

$$(2.7) \quad \begin{aligned} \frac{\delta(\zeta)}{\Delta t} \mathbf{U}(\mathbf{x}, \zeta) &= \mathcal{L}\mathbf{U}(\mathbf{x}, \zeta), & \mathbf{x} \in \mathbb{R}^d \setminus \bar{\Omega}, |\zeta| < 1, \\ \mathbf{U}(\mathbf{x}, \zeta) &= -\mathbf{U}^{\text{inc}}(\mathbf{x}, \zeta), & \mathbf{x} \in \Gamma, |\zeta| < 1, \end{aligned}$$

which, recalling that  $\mathbf{U}(\mathbf{x}, \zeta) = (\mathbf{u}(\mathbf{x}, \zeta), \mathbf{v}(\mathbf{x}, \zeta))$ , where

$$(2.8) \quad \frac{\delta(\zeta)}{\Delta t} \mathbf{v}(\mathbf{x}, \zeta) = \Delta \mathbf{u}(\mathbf{x}, \zeta), \quad \mathbf{x} \in \mathbb{R}^d \setminus \bar{\Omega}, |\zeta| < 1,$$

leads to the following Helmholtz boundary value problem

$$(2.9) \quad \begin{aligned} -\Delta \mathbf{u}(\mathbf{x}, \zeta) - \left( i \frac{\delta(\zeta)}{\Delta t} \right)^2 \mathbf{u}(\mathbf{x}, \zeta) &= 0, & \mathbf{x} \in \mathbb{R}^d \setminus \bar{\Omega}, |\zeta| < 1, \\ \mathbf{u}(\mathbf{x}, \zeta) &= -\mathbf{u}^{\text{inc}}(\mathbf{x}, \zeta), & \mathbf{x} \in \Gamma, |\zeta| < 1, \end{aligned}$$

for the complex wavenumber  $k(\zeta) = i \frac{\delta(\zeta)}{\Delta t}$ . Using an A-stable multistep method will ensure that the rational polynomial  $\delta$  satisfies  $\delta(\zeta) \in \mathbb{C}_+$  for  $\zeta \in \mathbb{C}_+$  [13, Section 1, p.131]. We are interested in the time-domain solution  $u(\mathbf{x}, t)$ , not in the Z-domain solution  $\mathbf{u}(\mathbf{x}, \zeta)$ . Both of them are related by means of the inverse Z-Transform, which corresponds to an application of the Cauchy integral formula:

$$(2.10) \quad u(\mathbf{x}, t_n) \approx u_n(\mathbf{x}) = \frac{1}{2\pi} \int_{\mathcal{C}} \frac{\mathbf{u}(\mathbf{x}, \zeta)}{\zeta^{n+1}} d\zeta, \quad \mathbf{x} \in \mathbb{R}^d \setminus \bar{\Omega}.$$

For implementation purposes, a good choice for the contour of integration  $\mathcal{C}$  is a circle of radius  $\lambda < 1$ , which allows the use of Fast Fourier Transform (FFT) to compute the integral approximately by means of a trapezoidal rule. Following [10, Section 4.2.1], the final expression is

$$(2.11) \quad \frac{1}{2\pi i} \int_{\mathcal{C}} \frac{1}{\zeta^{n+1}} \mathbf{u}(\mathbf{x}, \zeta) d\zeta \approx \frac{\lambda^{-n}}{N+1} \sum_{\ell=0}^N \mathbf{u}(\mathbf{x}, \zeta_{\ell}) \zeta_{\ell}^{-n}$$

where  $\zeta_{\ell} = e^{\frac{2\pi i \ell}{N+1}}$  and  $N \in \mathbb{N}$  is the number of quadrature points in the trapezoidal rule. This means that we need to solve  $N+1$  frequency domain problems (2.9) with  $\zeta = \zeta_{\ell}$ ,  $\ell = 0, \dots, N$  to approximate the solution of our wave equation. The order of convergence of this method is the same of the multistep method chosen. Due to Dahlquist's Barrier Theorem [17, Chapter V, Theorem 1.4], A-stable multistep methods are limited to order less than or equal to two, which is a major drawback of multistep based CQ.

**2.3. Multistage Convolution Quadrature.** There are A-stable implicit multistage methods of arbitrary order [1]. This is the main motivation for considering them for solving (2.2) instead of multistep methods. Letting  $A \in \mathbb{R}^{m \times m}$ ,  $\mathbf{b}, \mathbf{c} \in \mathbb{R}^m$  be the Butcher tableau for a given  $m$ -stage Runge-Kutta method, and defining the stages  $U_{nj}(\mathbf{x}) \approx U(\mathbf{x}, t_n + c_j \Delta t)$  and the steps  $U_n(\mathbf{x}) \approx U(\mathbf{x}, t_n)$ , the method amounts to computing a vector valued function

$$(2.12) \quad \begin{aligned} \underline{U}_n(\mathbf{x}) &:= (U_{n1}(\mathbf{x}), \dots, U_{nm}(\mathbf{x})) \\ &= (U(\mathbf{x}, t_n + c_1 \Delta t), \dots, U(\mathbf{x}, t_n + c_m \Delta t)), \quad n = 0, \dots, N, \end{aligned}$$

of stage solutions such that

$$(2.13) \quad \begin{aligned} \underline{U}_n &= U_n \mathbf{1} + \Delta t A \underline{\mathcal{L}} \underline{U}_n, \\ U_{n+1} &= U_n + \Delta t \mathbf{b} \cdot \underline{\mathcal{L}} \underline{U}_n. \end{aligned}$$

where  $\underline{\mathcal{L}} \underline{U}_n := (\mathcal{L}U_{n1}(\mathbf{x}), \dots, \mathcal{L}U_{nm}(\mathbf{x}))$ .

For stiffly accurate Runge-Kutta methods such as RadauIIA or LobattoIIIC families [15], we have the relation

$$\mathbf{e}_m^T A = \mathbf{b}^T,$$

where  $\mathbf{e}_m = (0, \dots, 0, 1) \in \mathbb{R}^m$ . Thus, the second equation in (2.13) can be derived from the first one by multiplying from the left by  $\mathbf{e}_m^T$ . Then, we can write

$$(2.14) \quad \underline{U}_n = \mathbf{1} \mathbf{e}_m^T \underline{U}_{n-1} + \Delta t A \underline{\mathcal{L}} \underline{U}_n,$$

The application of the Z-transform to the previous equation leads to the following equation in the Z-domain:

$$(2.15) \quad \underline{\mathbf{U}}(\zeta) = \zeta \mathbf{1} \mathbf{e}_m^T \underline{\mathbf{U}}(\zeta) + \Delta t A \underline{\mathcal{L}} \underline{\mathbf{U}}(\zeta),$$

denoting  $\underline{\mathbf{U}}(\zeta) := \sum_{n=0}^{\infty} \underline{U}_n \zeta^n = \sum_{n=0}^{\infty} ((u_{n1}(\mathbf{x}), v_{n1}(\mathbf{x})), \dots, (u_{nm}(\mathbf{x}), v_{nm}(\mathbf{x}))) \zeta^n$ .

From (2.15) we obtain the following expression

$$(2.16) \quad \frac{\delta^{\text{RK}}(\zeta)}{\Delta t} \underline{\mathbf{U}}(\zeta) = \underline{\mathcal{L}} \underline{\mathbf{U}}(\zeta),$$

where we wrote  $\boldsymbol{\delta}^{\text{RK}}(\zeta) := A^{-1}(I - \zeta \mathbf{1} e_m^T) \in \mathbb{C}^{m \times m}$ .

Similarly as for the multistep case, we derive a Helmholtz type equation with matrix wavenumber of complex coefficients. Letting  $\underline{\mathbf{U}} := ((\mathbf{u}_1, \mathbf{v}_1), \dots, (\mathbf{u}_m, \mathbf{v}_m))$ , we define  $\underline{\mathbf{u}} := (\mathbf{u}_1, \dots, \mathbf{u}_m)$  which satisfies

$$(2.17) \quad \begin{aligned} -\underline{\Delta} \underline{\mathbf{u}}(\mathbf{x}, \zeta) + \left( \frac{\boldsymbol{\delta}^{\text{RK}}(\zeta)}{\Delta t} \right)^2 \underline{\mathbf{u}}(\mathbf{x}, \zeta) &= 0, & \mathbf{x} \in \mathbb{R}^d \setminus \overline{\Omega}, \quad |\zeta| < 1, \\ \underline{\mathbf{u}}(\mathbf{x}, \zeta) &= -\underline{\mathbf{u}}^{\text{inc}}(\mathbf{x}, \zeta), & \mathbf{x} \in \Gamma, \quad |\zeta| < 1, \end{aligned}$$

where  $\underline{\Delta} \underline{\mathbf{u}}(\mathbf{x}, \zeta) := (\Delta \mathbf{u}_1(\mathbf{x}, \zeta), \dots, \Delta \mathbf{u}_m(\mathbf{x}, \zeta))$ . The system can be decoupled by diagonalization of the matrix-valued wavenumber  $\boldsymbol{\delta}^{\text{RK}}(\zeta) = P(\zeta)D(\zeta)P^{-1}(\zeta)$ , where  $D(\zeta) = \text{diag}(\delta_1^{\text{RK}}(\zeta), \dots, \delta_m^{\text{RK}}(\zeta))$  and  $P(\zeta) \in \mathbb{C}^{m \times m}$  are the matrices of eigenvalues and eigenvectors of  $\boldsymbol{\delta}^{\text{RK}}(\zeta)$ , respectively. Finally, we need to solve for  $j = 1, \dots, m$

$$(2.18) \quad \begin{aligned} -\Delta \mathbf{w}_j(\mathbf{x}, \zeta) - \left( i \frac{\delta_j^{\text{RK}}(\zeta)}{\Delta t} \right)^2 \mathbf{w}_j(\mathbf{x}, \zeta) &= 0, & \mathbf{x} \in \mathbb{R}^d \setminus \overline{\Omega}, \quad |\zeta| < 1, \\ \mathbf{w}_j(\mathbf{x}, \zeta) &= -\mathbf{w}_j^{\text{inc}}(\mathbf{x}, \zeta), & \mathbf{x} \in \Gamma, \quad |\zeta| < 1, \end{aligned}$$

where we have used the change of variables  $\mathbf{w}(\mathbf{x}, \zeta) = P^{-1}(\zeta)\underline{\mathbf{u}}(\mathbf{x}, \zeta)$ . As regards implementation, the procedure follows exactly as in (2.11), using the FFT and solving a finite number of Helmholtz problems.

**2.4. Method of Fundamental Solutions.** In the previous section we reduced the time domain wave equation with Dirichlet boundary conditions to multiple Helmholtz equations with Dirichlet conditions, by means of the Z transform. Different solvers in the frequency domain can be used for these boundary value problems (BVPs). Here we focus on the Method of Fundamental Solutions. We are interested in solving either the interior or exterior Helmholtz Dirichlet BVP with wavenumber  $k \in \mathbb{C}_+$  and Dirichlet boundary conditions, i.e.

$$(2.19) \quad \begin{aligned} -\Delta u(\mathbf{x}) - k^2 u(\mathbf{x}) &= 0, & \mathbf{x} \in \Omega, \\ u(\mathbf{x}) &= g(\mathbf{x}), & \mathbf{x} \in \Gamma \end{aligned}$$

for the interior problem, or

$$(2.20) \quad \begin{aligned} -\Delta u(\mathbf{x}) - k^2 u(\mathbf{x}) &= 0, & \mathbf{x} \in \mathbb{R}^d \setminus \overline{\Omega}, \\ u(\mathbf{x}) &= g(\mathbf{x}), & \mathbf{x} \in \Gamma \\ &+ \text{Radiation Conditions} \end{aligned}$$

for the exterior problem. In both cases,  $g$  is a function defining Dirichlet boundary conditions, modeling an incident field (plane-wave or point source).

The fundamental solution for the Helmholtz equation in  $\mathbb{R}^2$  is the Hankel function of the first kind and order zero

$$(2.21) \quad G(\mathbf{x} - \mathbf{y}; k) = \frac{i}{4} H_0^{(1)}(k|\mathbf{x} - \mathbf{y}|), \quad \mathbf{x} \neq \mathbf{y}.$$

The Method of Fundamental Solutions (MFS) consists in selecting a finite set of points  $\{\mathbf{y}_j\}_{j=1}^N$  and writing  $\tilde{u}$  as a linear combination of fundamental solutions centered at these points

$$(2.22) \quad \tilde{u}(\mathbf{x}) = \sum_{j=1}^{N_y} \alpha_j G(\mathbf{x} - \mathbf{y}_j; k), \quad \mathbf{x} \in \mathbb{R}^2 \setminus \overline{\Omega},$$

with coefficients  $\alpha_j \in \mathbb{C}$ ,  $j = 1, \dots, N_y$ . The charge locations  $\{\mathbf{y}_j\}$  are chosen on a smooth curve contained in the domain  $\Omega$  for exterior problems, and enclosing  $\Omega$  for interior problems (see Figure 1). In 2D, exponential convergence can be achieved if these are suitably chosen for analytic domains [3]. The optimal placement of auxiliary sources is still an unsolved problem in 3D.

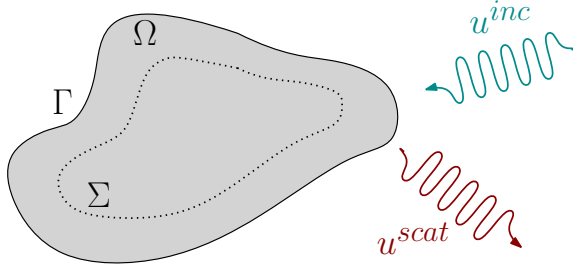


Fig. 1: Example geometry with charge points inside  $\Omega$  on curve  $\Sigma$ .

The coefficients can be determined by  $L^2(\Gamma)$ -fitting of the known boundary data  $g$ . We need to find coefficients  $\alpha_j$ ,  $j = 1, \dots, N$  such that

$$(2.23) \quad (\alpha_1, \dots, \alpha_N) = \operatorname{argmin}_{\alpha \in \mathbb{C}^N} \|\tilde{u} - g\|_{L^2(\Gamma)}.$$

This can be done by choosing collocation points  $\mathbf{x}_\ell$ ,  $\ell = 1, \dots, M$ , to approximate the  $L^2$ -norm on the boundary. Then, the problem can be solved by a least squares method, enforcing the Dirichlet boundary conditions. We can rewrite it in matrix form as

$$(2.24) \quad \alpha^* = \operatorname{argmin}_{\alpha \in \mathbb{C}^N} \|\mathbb{M}\alpha - \mathbf{g}\|_2.$$

where  $\alpha = (\alpha_1, \dots, \alpha_{N_y})^T$ ,  $\mathbf{g} = (g(\mathbf{x}_1), \dots, g(\mathbf{x}_{N_x}))^T$  and  $\mathbb{M}_{\ell j} = G(\mathbf{x}_\ell - \mathbf{y}_j; k)$  for  $\ell = 1, \dots, N_x$ ,  $j = 1, \dots, N_y$ .

**3. Algorithm.** We denote

$$(3.1) \quad \mathbb{M}(\zeta) := \begin{pmatrix} G(\mathbf{x}_0 - \mathbf{y}_0; \zeta) & \dots & G(\mathbf{x}_0 - \mathbf{y}_{N_y}; \zeta) \\ \vdots & \dots & \vdots \\ G(\mathbf{x}_{N_x} - \mathbf{y}_0; \zeta) & \dots & G(\mathbf{x}_{N_x} - \mathbf{y}_{N_y}; \zeta) \end{pmatrix} \in \mathbb{C}^{N_x \times N_y}$$

the matrix related to the minimization problem arising from the MFS (2.23). Note that this is a dense matrix. For the two dimensional Helmholtz equation over a domain  $\Omega \subset \mathbb{R}^2$  with analytic boundary let  $\Phi : \mathbb{C} \rightarrow \mathbb{C}$  be such that

$$(3.2) \quad \Gamma := \{\mathbf{x} \in \mathbb{R}^2 : \mathbf{x} = (\operatorname{Re} \Phi(z), \operatorname{Im} \Phi(z)), \quad z \in \mathbb{C}, \quad |z| = 1\}$$

and

$$(3.3) \quad \Sigma := \{\mathbf{x} \in \mathbb{R}^2 : \mathbf{x} = (\operatorname{Re} \Phi(z), \operatorname{Im} \Phi(z)), \quad z \in \mathbb{C}, \quad |z| = r\}$$

are the boundary  $\Gamma$  of the domain  $\Omega$  and the curve  $\Sigma$  where charge points are chosen, respectively. This was proposed for the Laplace problem [11] and has been used for Helmholtz problems too.

In [3] a different approach is suggested to improve results in the presence of singularities in the parametrizations of analytic domains, but for simplicity we decided not to use it, because we are interested in testing the direct coupling of CQ and MFS. We present the algorithms for the multistep and multistage case. The CQ implementation is mainly based on the presentation given in [10, Sections 4 and 6]. It is worth mentioning that a scaling of the data is needed in order to correctly compute the Z-Transform of boundary data and the inverse Z-Transform as a contour integral over a circle of radius  $0 < \lambda < 1$  [10, Section 4.2]. Evaluating Z-Transforms at points  $\zeta_m = \lambda \exp\left(\frac{2im\pi}{M+1}\right)$  is equivalent to computing the Discrete Fourier Transform (DFT) of scaled functions:

$$(3.4) \quad \sum_{n=0}^M g(\mathbf{x}_\ell, t_n) \zeta_m^n = \sum_{n=0}^M \{\lambda^n g(\mathbf{x}_\ell, t_n)\} \exp\left(\frac{2imn\pi}{M+1}\right).$$

Also, computing the approximate contour integral of the inverse Z-Transform (2.11) is equivalent to computing an inverse DFT and rescaling the output:

$$(3.5) \quad u(\mathbf{x}_\ell, t_n) \approx \frac{\lambda^{-n}}{N+1} \sum_{\ell=0}^M \mathbf{u}(\mathbf{x}, \zeta_\ell) \zeta_\ell^{-n} = \lambda^{-n} \left( \frac{1}{M+1} \sum_{\ell=0}^M \mathbf{u}(\mathbf{x}, \zeta_\ell) \exp\left(\frac{-2i\ell n\pi}{M+1}\right) \right).$$

Observe that this involves using the same number of quadrature points for the trapezoidal rule in (2.11) as the number of discrete times  $t_n, n = 0, \dots, M$ . As we are dealing with analytic functions (Helmholtz solutions for  $k \in \mathbb{C}_+$ ) this is not a problem, as exponential convergence is guaranteed for the trapezoidal rule. Nevertheless, some experiments have shown that accuracy can be lost in presence of cavities, due to the appearance of so-called scattering poles [4], requiring to overresolve in the frequency domain.

Now, we proceed to detail the algorithms used for the multistep and multistage CQ + MFS. The computational complexity of these algorithms is mainly due to solving the linear system by a least squares method. Boundary data can be stored in a matrix of size  $N_x \times M$ . The cost of computing the DFT by means of the FFT is negligible compared to the other steps. The assembly of a single matrix requires  $\mathcal{O}(N_x N_y)$  operations, because it is based in evaluations over charge and collocation points. The least squares problem is solved by the QR method for a dense matrix, sparse QR for a sparse matrix (based on Matlab's backslash operator) which is the most costly operation in the algorithm. This is repeated  $M$  times, where  $M$  is the number of timesteps. For the case of Runge-Kutta methods, this has to be multiplied by the number of stages  $S$ .

**Multistep CQ - MFS**

a) We define  $\lambda = \epsilon^{1/2M}$  and  $\Delta t = T/M$ .

b) For a given parametrization  $\Phi : \mathbb{C} \mapsto \mathbb{C}$  and  $r \in (0, 1)$  we compute

$$(3.6) \quad \begin{aligned} \mathbf{x}_\ell &= (\operatorname{Re} \Phi(z_\ell), \operatorname{Im} \Phi(z_\ell)), & z_\ell &= \exp\left(\frac{2i\ell\pi}{N_x+1}\right), \quad \ell = 0, \dots, N_x, \\ \mathbf{y}_j &= (\operatorname{Re} \Phi(rz_j), \operatorname{Im} \Phi(rz_j)), & z_j &= \exp\left(\frac{2ij\pi}{N_y+1}\right), \quad \ell = 0, \dots, N_y. \end{aligned}$$

c) We compute the data

$$(3.7) \quad g(\mathbf{x}_\ell, t_m) = -u^{\text{inc}}(\mathbf{x}_\ell, t_m), \quad \ell = 0, \dots, N_x, \quad m = 0, \dots, M.$$

d) We rescale the data:

$$(3.8) \quad h_m(\mathbf{x}_\ell) = \lambda^m g(\mathbf{x}_\ell, t_m), \quad \ell = 0, \dots, N_x, \quad m = 0, \dots, M.$$

e) Compute the DFT of the scaled data  $\{h_m(\mathbf{x}_\ell)\}_{m=0}^M$ ,  $\ell = 0, \dots, N_x$  to obtain

$$(3.9) \quad \{\tilde{h}_m(\mathbf{x}_\ell)\}_{m=0}^M, \quad \ell = 0, \dots, N_x.$$

f) For each  $m = 0, \dots, M$ , solve the least squares problem to obtain the vector of coefficients:

$$(3.10) \quad \boldsymbol{\alpha}^*(\zeta_m) = \operatorname{argmin}_{\boldsymbol{\alpha} \in \mathbb{C}^{N_y+1}} \left\| \mathbb{M}(\delta(\zeta_m)/\Delta t) \boldsymbol{\alpha} - \tilde{\mathbf{h}}_m \right\|_2$$

where  $\boldsymbol{\alpha} := (\alpha_0 \quad \dots \quad \alpha_{N_y})^T$ ,  $\tilde{\mathbf{h}}_m := (\tilde{h}_m(\mathbf{x}_0) \quad \dots \quad \tilde{h}_m(\mathbf{x}_{N_x}))^T$  and  $\mathbb{M}(\delta(\zeta_m)/\Delta t)$  is defined by (3.1).

g) We evaluate the solutions in a set of points of interest  $\{\mathbf{p}_l\}_{l=0}^{N_p}$

$$(3.11) \quad \tilde{v}_m(\mathbf{p}_l) = \sum_{j=0}^{N_y} \alpha_j^*(\zeta_m) G(\mathbf{p}_l - \mathbf{y}_j; k_m)$$

to obtain the vector  $\tilde{\mathbf{v}}_m = (\tilde{v}_m(\mathbf{p}_0) \quad \dots \quad \tilde{v}_m(\mathbf{p}_{N_p}))^T$

h) We compute the inverse DFT over the rows of the matrix  $\tilde{\mathbf{v}} = (\tilde{\mathbf{v}}_0 \quad \dots \quad \tilde{\mathbf{v}}_M)$  to obtain

$$(3.12) \quad \mathbf{v} = (\mathbf{v}_0 \quad \dots \quad \mathbf{v}_M).$$

i) Finally, we rescale the solution

$$(3.13) \quad u(\mathbf{p}_l, t_m) \approx \lambda^{-m} v_m(\mathbf{p}_l), \quad l = 0, \dots, N_p, \quad m = 0, \dots, M.$$

**Multistage CQ - MFS**

a) We define  $\lambda = \epsilon^{1/2M}$  and  $\Delta t = T/M$ .

b) For a given parametrization  $\Phi : \mathbb{C} \mapsto \mathbb{C}$  and  $r \in (0, 1)$  we compute:

$$\mathbf{x}_\ell \text{ for } \ell = 0, \dots, N_x, \quad \mathbf{y}_j \text{ for } j = 0, \dots, N_y.$$

c) We compute the data for each stage  $s = 1, \dots, S$

$$(3.14) \quad g(\mathbf{x}_\ell, t_m + c_s \Delta t) = -u^{\text{inc}}(\mathbf{x}_\ell, t_m + c_s \Delta t), \quad \ell = 0, \dots, N_x, \quad m = 0, \dots, M.$$

d) We rescale the data:

$$(3.15) \quad h_{m,s}(\mathbf{x}_\ell) = \lambda^m g(\mathbf{x}_\ell, t_m + c_s \Delta t), \quad \ell = 0, \dots, N_x, \quad m = 0, \dots, M.$$

e) Compute the DFT of the scaled data  $\{h_{m,s}(\mathbf{x}_\ell)\}_{m=0}^M$ ,  $\ell = 0, \dots, N_x$ ,  $s = 1, \dots, S$  to obtain

$$(3.16) \quad \{\tilde{h}_{m,s}(\mathbf{x}_\ell)\}_{m=0}^M, \quad \ell = 0, \dots, N_x, \quad s = 1, \dots, S.$$

f) For each  $m = 0, \dots, M$  we compute the kronecker product

$$P^{-1}(\zeta_m) \otimes \tilde{\mathbf{h}}_m = \boldsymbol{\nu}_m = (\boldsymbol{\nu}_{m,1}, \dots, \boldsymbol{\nu}_{m,S})$$

and for  $s = 1, \dots, S$  we solve the least squares problem to obtain the vector of coefficients:

$$(3.17) \quad \boldsymbol{\alpha}_s^*(\zeta_m) = \operatorname{argmin}_{\boldsymbol{\alpha} \in \mathbb{C}^{N_y+1}} \|\mathbb{M}(\delta_s^{\text{RK}}(\zeta_m)/\Delta t)\boldsymbol{\alpha} - \boldsymbol{\nu}_{m,s}\|_2$$

where

$$\boldsymbol{\alpha} := (\alpha_0, \dots, \alpha_{N_y})^T,$$

$$\tilde{\mathbf{h}}_m := (\tilde{h}_{m,1}(\mathbf{x}_0), \dots, \tilde{h}_{m,1}(\mathbf{x}_{N_x}), \dots, \tilde{h}_{m,S}(\mathbf{x}_0), \dots, \tilde{h}_{m,S}(\mathbf{x}_{N_x}))^T$$

and  $\mathbb{M}(\delta_s^{\text{RK}}(\zeta_m)/\Delta t)$  is defined by (3.1).

g) We evaluate the solutions in a set of points of interest  $\{\mathbf{p}_l\}_{l=0}^{N_p}$

$$(3.18) \quad \tilde{v}_{m,s}(\mathbf{p}_l) = \sum_{j=0}^{N_y} \alpha_{j,s}^*(\zeta_m) G(\mathbf{p}_l - \mathbf{y}_j; i\delta_s^{\text{RK}}(\zeta_m)/\Delta t)$$

to obtain the vector  $\tilde{\mathbf{v}}_{m,s} = (\tilde{v}_{m,s}(\mathbf{p}_0) \dots \tilde{v}_{m,s}(\mathbf{p}_{N_p}))^T$

h) We compute the kronecker product

$$P(\zeta_m) \otimes (\tilde{\mathbf{v}}_{m,1}, \dots, \tilde{\mathbf{v}}_{m,S}) = \tilde{\tilde{\mathbf{v}}}_m$$

i) We compute the inverse DFT over the rows of the matrix  $\mathbf{V}_s = (\tilde{\tilde{\mathbf{v}}}_{0,s} \dots \tilde{\tilde{\mathbf{v}}}_{M,s})$  to obtain

$$(3.19) \quad \mathbf{v}_s = (\mathbf{v}_{0,s} \dots \mathbf{v}_{M,s}).$$

j) Finally, we rescale the solution

$$(3.20) \quad u(\mathbf{p}_l, t_m + \Delta t) \approx \lambda^{-m} v_{m,S}(\mathbf{p}_l), \quad l = 0, \dots, N_p, \quad m = 0, \dots, M.$$

**4. Numerical Experiments.** For all of our examples we will consider an incident field consisting of a plane wave, i.e. for a given  $\mathbf{d} \in \mathbb{R}^2$  the incident field  $u^{\text{inc}}$  corresponds to

$$(4.1) \quad u^{\text{inc}}(\mathbf{x}, t) := f(t - t_{\text{lag}} - \mathbf{d} \cdot \mathbf{x})$$

where

$$(4.2) \quad f(t) := \sin(\omega t)\mu(t)\mu(4-t), \quad \mu(t) := \frac{\exp(-\beta t)}{1 + \exp(-\beta t)}, \quad \beta = 5, \quad \omega = 4.$$

The errors are measured considering a relative pointwise error in space,  $L^2$ -norm in time:

$$(4.3) \quad \text{error} := \frac{\left( \sum_{n=0}^N \sum_{\mathbf{x} \in X} |u(\mathbf{x}, t_n) - \tilde{u}(\mathbf{x}, t_n)|^2 \right)^{1/2}}{\left( \sum_{n=0}^N \sum_{\mathbf{x} \in X} |u(\mathbf{x}, t_n)|^2 \right)^{1/2}},$$

where  $X \subset \mathbb{R}^2 \setminus \Omega$  is a finite set.

Multistep CQ is tested in two cases, backward differentiation formulas (BDF) of order 1 and 2. Those are fully represented by the following polynomials

$$(4.4) \quad \delta^{\text{BDF1}}(\zeta) = 1 - \zeta, \quad \delta^{\text{BDF2}}(\zeta) = \frac{1}{2}(\zeta^2 - 4\zeta + 3).$$

Multistage CQ is tested with RadauIIA family, considering methods of two and three stages respectively. The Butcher tableau is given by

$$(4.5) \quad A = \begin{pmatrix} 5/12 & -1/12 \\ 3/4 & 1/4 \end{pmatrix}, \quad \mathbf{b}^T = \mathbf{e}_m^T A, \quad \mathbf{c} = A\mathbf{1},$$

for the two-stage method, and

$$(4.6) \quad A = \begin{pmatrix} 11/45 & 37/225 & -2/225 \\ 37/225 & 11/45 & -2/225 \\ 4/9 & 4/9 & 1/9 \end{pmatrix} + \begin{pmatrix} -7\frac{\sqrt{6}}{360} & -169\frac{\sqrt{6}}{1800} & \frac{\sqrt{6}}{75} \\ 169\frac{\sqrt{6}}{1800} & 7\frac{\sqrt{6}}{360} & -\frac{\sqrt{6}}{75} \\ -\frac{\sqrt{6}}{36} & \frac{\sqrt{6}}{36} & 0 \end{pmatrix}, \quad \mathbf{b}^T = \mathbf{e}_m^T A, \quad \mathbf{c} = A\mathbf{1},$$

for the three-stage method. RadauIIA families have classical order of convergence of  $2m + 1$ , stage order of convergence of  $m$ , where  $m$  is the number of stages [17].

To take advantage of the exponentially decaying nature of the fundamental solutions, we discard terms of matrix (3.1) that are below a given tolerance of  $1e-20$  as it was done in [6]. This allows

us to use sparse linear solvers for most of our least squares problems, without losing accuracy. Our implementation is carried out in Matlab 2018a using the backslash operator, which solves the least squares problem by the QR method. For the case of sparse matrices, it automatically uses the sparse QR method.

**4.1. Method of Fundamental Solutions for complex wavenumbers.** First, we need to validate that the method behaves correctly in this different setting. We show exponential convergence for the MFS for several complex wavenumbers. The problem studied is

$$(4.7) \quad \begin{aligned} -\Delta u(\mathbf{x}) - k^2 u(\mathbf{x}) &= 0 && \text{in } \mathbb{R}^2 \setminus \Omega, \\ u(\mathbf{x}) &= -u^{\text{inc}}(\mathbf{x}) && \text{on } \Gamma, \\ &+ \text{Radiation Conditions} \end{aligned}$$

where  $\Omega$  is the unit disk and charge points are chosen on a circle of radius  $r = 0.8$ . The incident field  $u^{\text{inc}}(\mathbf{x})$  corresponds to

$$(4.8) \quad u^{\text{inc}}(\mathbf{x}) = \frac{i}{4} H_0^{(1)}(k|\mathbf{x} - \mathbf{x}_{\text{src}}|), \quad \mathbf{x} \in \mathbb{R}^2,$$

where  $\mathbf{x}_{\text{src}} = (0.2, 0.3)$ . As this is an exterior problem and we are locating a source in the interior of the domain, the exact solution for the problem is  $u(\mathbf{x}) = -u^{\text{inc}}(\mathbf{x})$  in the exterior of  $\Omega$ .

The number of collocation points is  $N = 600$  for each problem. Convergence results for the numerical experiments are shown in Figure 2.

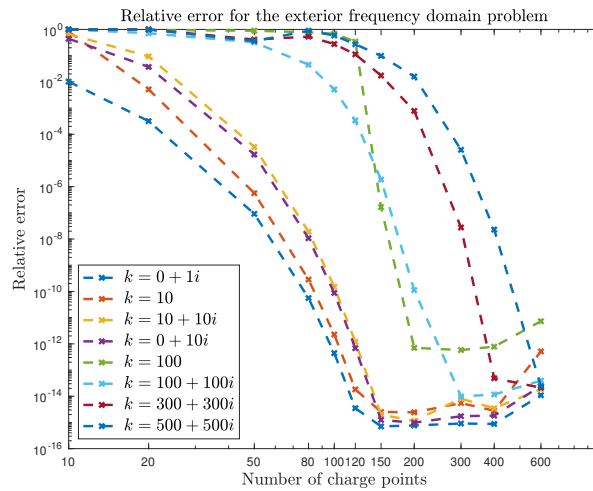


Fig. 2: Convergence results for the exterior Helmholtz problem of Section 4.1 with different wavenumbers.

**4.2. Scattering at a disk.** Our first example consists in solving the interior problem of acoustic scattering at a disk of unit radius. The incident field is the planewave defined in (4.1). We solve the interior problem with Dirichlet boundary conditions, for which we expect as a solution

$$(4.9) \quad u(\mathbf{x}, t) = u^{\text{inc}}(\mathbf{x}, t), \quad \mathbf{x} \in \mathbb{R}^2 \setminus \Omega.$$

The speed of propagation of the wave is always set to  $c = 1$  and the final time of computation is  $T = 10$ .

The geometry is shown in Figure 3, meanwhile convergence of BDF1, BDF2 and RadauIIA Runge-Kutta methods is presented in Figure 4a. The number of collocation points and charges are chosen as rather large  $N_x = 2000, N_y = 1000$  to have errors mainly due to the time discretization and not by the spatial error due to the MFS. Charges are located in a circle of radius  $r = 1.2$ . The solution is computed at  $X = \{(-0.5, -0.5), (-0.5, 0.5), (0.5, 0.5), (0.5, -0.5)\}$ . We also solve the exterior problem and compare our results with respect to an overkill solution based on three stages RadauIIA method with  $M = 1600$ . The radius used for the curve  $\Sigma$  is  $r = 0.8$  and the solution is computed in  $X = \{(-2, -2), (-2, 2), (2, 2), (2, -2)\}$ . Results are shown in Figure 4b. Both experiments show that it is possible to obtain the classical order of convergence of each multistep and multistage method, although for the interior problem a limited accuracy is reached, which was not possible to improve by increasing the number of charges. This can be explained by the limited accuracy that in general is achievable by the CQ method [10]. We also illustrate the percentage of matrix entries dropped due to sparsification in Figure 6, for BDF2 based CQ with 1600 timesteps.

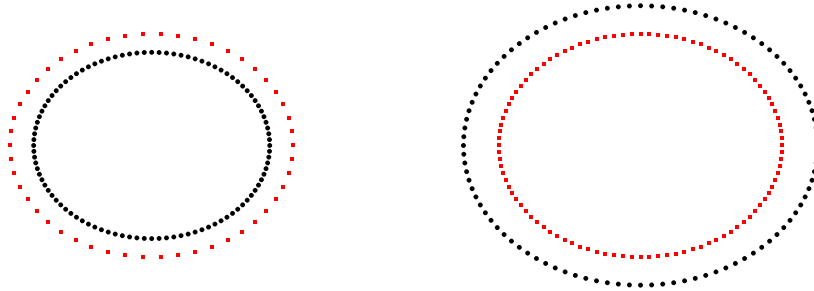
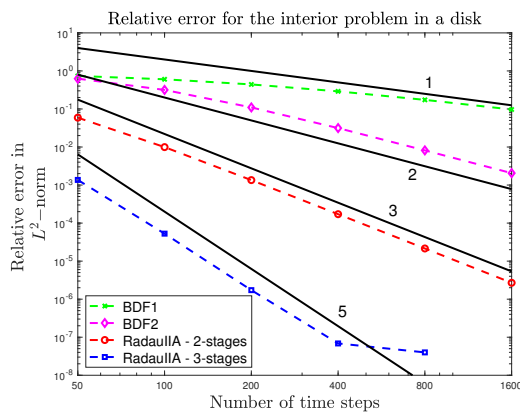
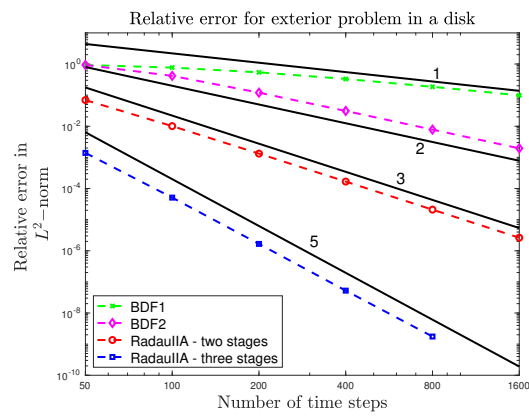


Fig. 3: Circle. Collocation points are marked as black circles, while charge points are marked as red squares. Interior and exterior problem, respectively.



(a) Interior problem.



(b) Exterior problem.

Fig. 4: Convergence of the CQ scheme for the interior/ exterior problem in Section 4.2, compared with an (a) exact solution; (b) overkill solution.

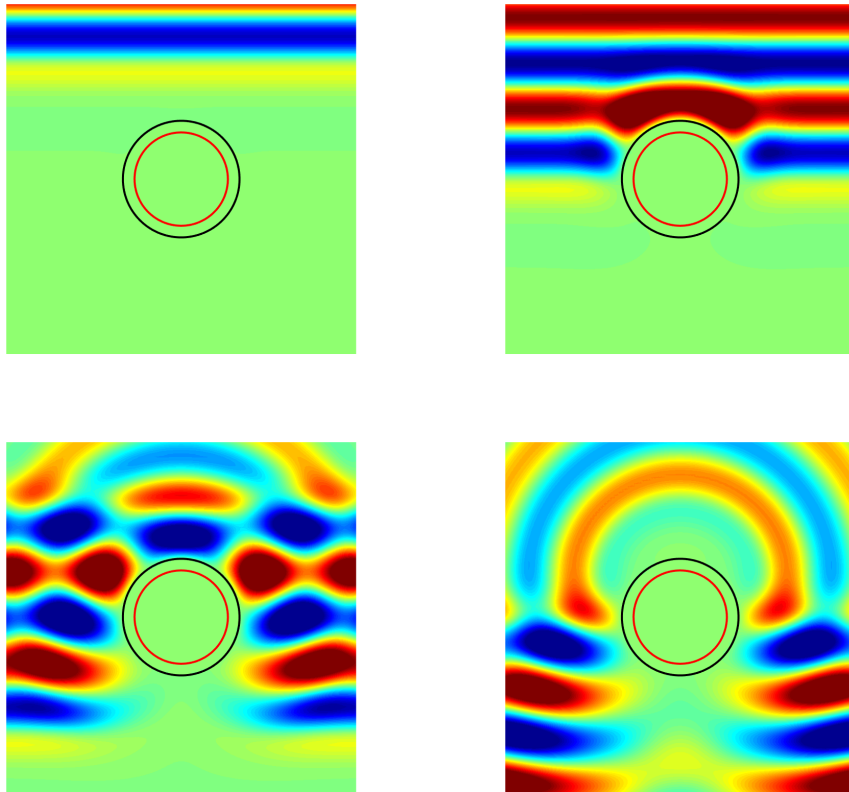


Fig. 5: Snapshots of the solution to the exterior problem in  $[-3, 3] \times [-3, 3]$  at times  $t = 2, 4, 6$  and  $8$ .

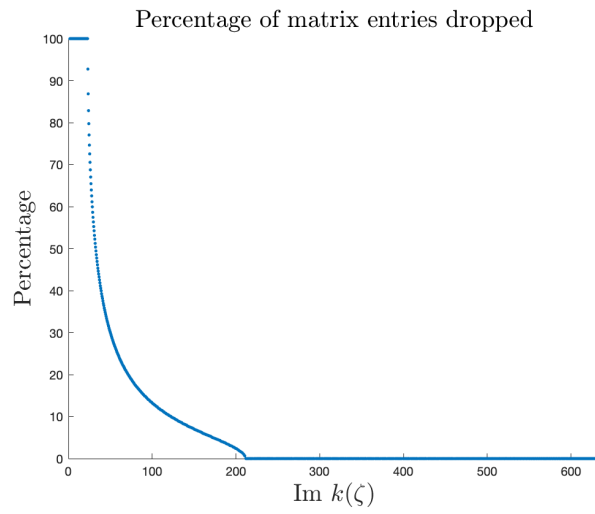


Fig. 6: Percentage of matrix entries (3.1) from experiment in Section 4.2 dropped due to sparsification with tolerance  $10^{-20}$  for BDF2 CQ with  $M = 1600$ .

**4.3. Scattering at a rounded triangle.** We repeat the example of the previous section but with a different geometry. Now we consider a rounded triangle, which can be parametrized for  $s \in [0, 2\pi]$

$$(4.10) \quad x(s) + iy(s) = e^{is} + a_1 e^{-2is}, \quad a_1 = 0.3.$$

The complexification of this can be seen as  $\Phi(z) = z + \frac{a_1}{z^2}$ ,  $z \in \mathbb{C}$ . If we restrict  $\Phi$  to the unit circle we obtain  $\Phi(e^{is}) = x(s) + iy(s)$ . We define our geometries of interest by

$$(4.11) \quad \Gamma := \{(x, y) \in \mathbb{R}^2 : x = x(s), y = y(s), \Phi(e^{is}) = x(s) + iy(s) \text{ for } s \in [0, 2\pi]\}$$

and

$$(4.12) \quad \Sigma := \{(x, y) \in \mathbb{R}^2 : x = x(s), y = y(s), \Phi(re^{is}) = x(s) + iy(s) \text{ for } s \in [0, 2\pi]\},$$

with the radius  $r = 1.2$  for the interior problem and  $r = 0.85$  for the exterior problem. These geometries are shown in Figure 7. Numerical results for this experiment are the same as for the unit circle, choosing fixed values  $N = 2000, N_p = 1000$ . The solution was computed in  $X = \{(-0.5, -0.5), (-0.5, 0.5), (0, 0), (0.5, 0)\}$  for the interior problem and  $X = \{(-2, -2), (-2, 2), (2, 2), (2, -2)\}$  for the exterior problem. Results are shown in Figures 8a and 8b.

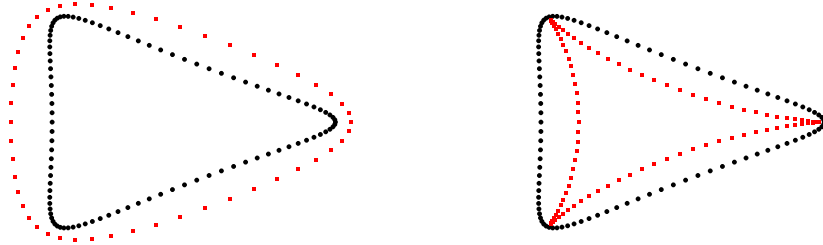
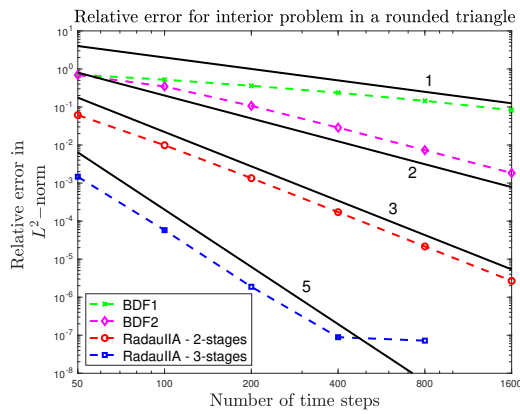
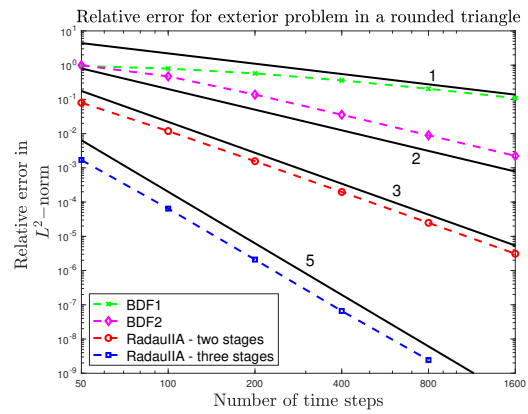


Fig. 7: Rounded triangle. Collocation points are marked as black circles, while charge points are marked as red squares. Interior and exterior problem, respectively.



(a) Interior problem.



(b) Exterior problem.

Fig. 8: Convergence of the CQ scheme for the interior/interior problem in Section 4.3, compared with an (a) exact solution; (b) overkill solution.

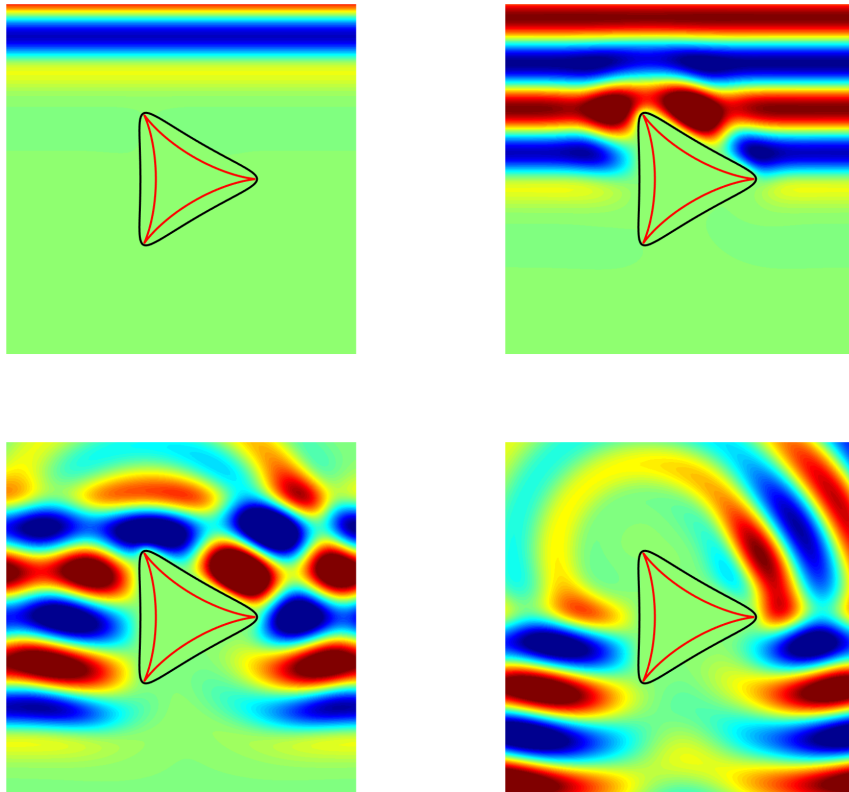


Fig. 9: Snapshots of the solution to the exterior problem in  $[-3, 3] \times [-3, 3]$  at times  $t = 2, 4, 6$  and  $8$ .

**4.4. Scattering at an inverted ellipse.** We repeat the example with an inverted ellipse, which can be parametrized for  $s \in [0, 2\pi]$

$$(4.13) \quad x(s) + iy(s) = \frac{e^{is}}{1 + a_2 e^{2is}}, \quad a_2 = 0.25.$$

The complexification of this can be seen as  $\Phi(z) = \frac{z}{1 + a_2 z^2}$ ,  $z \in \mathbb{C}$ . If we restrict  $\Phi$  to the unit circle we obtain  $\Phi(e^{is}) = x(s) + iy(s)$ . We define our geometries of interest by

$$(4.14) \quad \Gamma := \{(x, y) \in \mathbb{R}^2 : x = x(s), y = y(s), \Phi(e^{is}) = x(s) + iy(s) \text{ for } s \in [0, 2\pi]\}$$

and

$$(4.15) \quad \Sigma := \{(x, y) \in \mathbb{R}^2 : x = x(s), y = y(s), \Phi(re^{is}) = x(s) + iy(s) \text{ for } s \in [0, 2\pi]\},$$

with the radius  $r = 1.2$  for the interior problem and  $r = 0.8$  for the exterior problem. These geometries are shown in Figure 10. Numerical results for this experiment are the same as for the unit circle, choosing fixed values  $N = 2000, N_p = 1000$ . The solution is computed in  $X = \{(-0.5, -0.5), (-0.5, 0.5), (0.5, 0.5), (0.5, -0.5)\}$  for the interior problem,  $X = \{(-2, -2), (-2, 2), (2, 2), (2, -2)\}$  for the exterior problem. Errors are shown in Figures 11a and 11b.

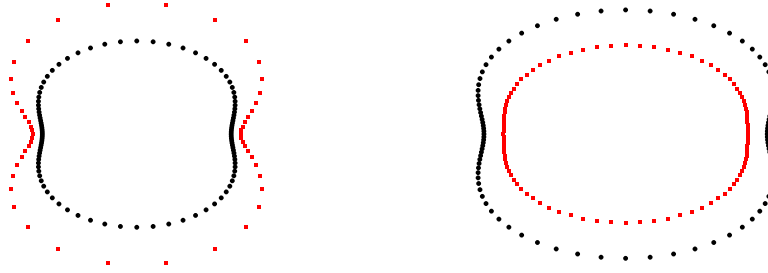


Fig. 10: Inverted Ellipse. Collocation points are marked as black circles, while charge points are marked as red squares. Interior and exterior problems, respectively.

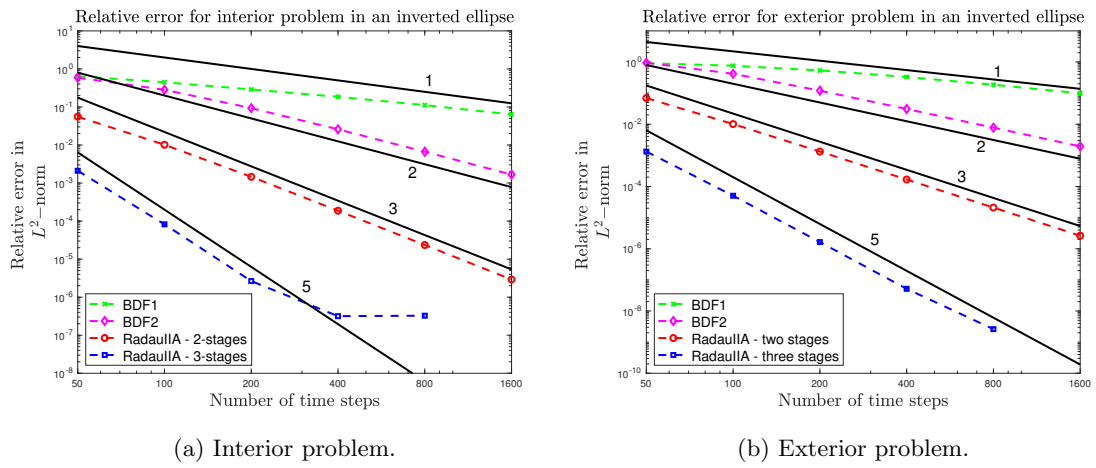


Fig. 11: Convergence of the CQ scheme for the interior/ exterior problem in Section 4.4, compared with an (a) exact solution; (b) overkill solution.

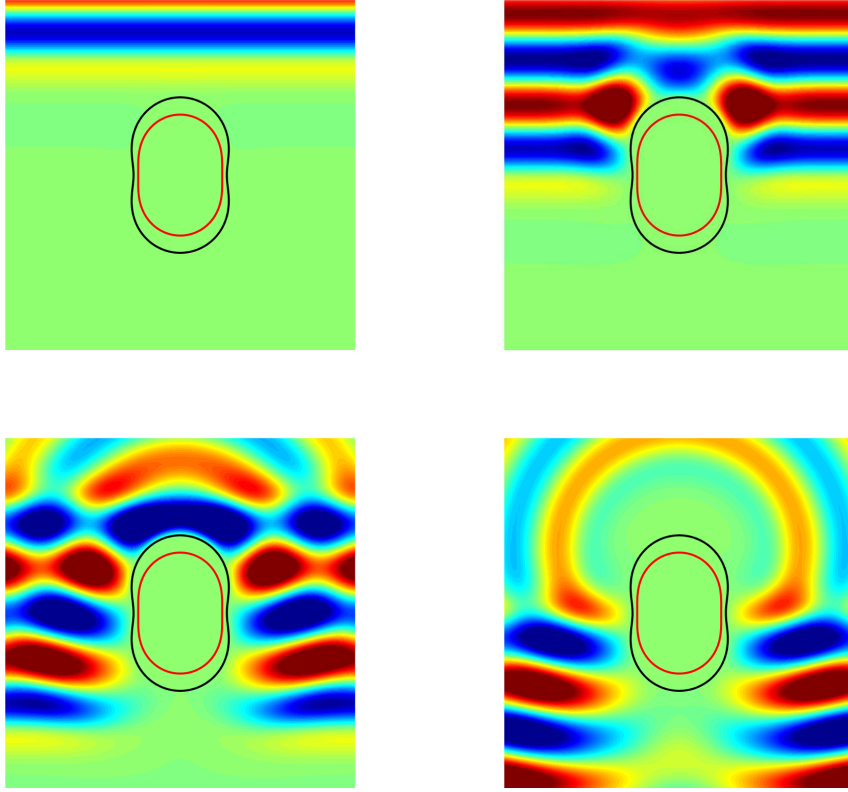


Fig. 12: Snapshots of the solution to the exterior problem in  $[-3, 3] \times [-3, 3]$  at times  $t = 2, 4, 6$  and  $8$ .

**5. Conclusions.** Throughout this article we worked with the Convolution Quadrature methods in combination with the Method of Fundamental Solutions as a frequency domain solver. Our numerical experiments over analytic domains show that both methods fit well together. We obtain classical order of convergence for multistep and multistage methods at interior and exterior problems. The nature of fundamental solutions of Helmholtz problems with complex wavenumbers suits well for these coupling too. These functions are exponentially decaying for the case  $s \in \mathbb{C}_+$ , which gives us the opportunity to discard terms below a given tolerance. The result is a sparse linear system which is much more efficient to solve than the original determined by a dense matrix. Our computations show that this procedure is effective for the problems studied while considering a tolerance below  $10^{-20}$ .

MFS is a representative of a larger class of Trefftz methods. A generalization is the Multiple Multipole Method [8]. It has been successfully used in 3D in frequency domain based on heuristics for the placement of multipoles [9]. This work offers a proof of concept that CQ can be used to transfer these techniques to time domain.

## REFERENCES

- [1] L. BANJAI, C. LUBICH, AND J. M. MELENK, *Runge–Kutta Convolution Quadrature for operators arising in Wave propagation*, Numerische Mathematik, 119 (2011), pp. 1–20.
- [2] L. BANJAI AND S. SAUTER, *Rapid Solution of the Wave Equation in Unbounded Domains*, SIAM Journal on Numerical Analysis, 47 (2008), pp. 227–249.
- [3] A. H. BARNETT AND T. BETCKE, *Stability and convergence of the Method of Fundamental Solutions for Helmholtz problems on analytic domains*, Journal of Computational Physics, 227 (2008), pp. 7003–7026.
- [4] T. BETCKE, N. SALLES, AND W. SMIGAJ, *Overresolving in the Laplace Domain for Convolution Quadrature methods*, SIAM Journal on Scientific Computing, 39 (2017), pp. A188–A213.
- [5] S. BÖRM, M. LOPEZ-FERNANDEZ, AND S. SAUTER, *Variable Order, Directional H2-Matrices for Helmholtz Problems with Complex Frequency*, arXiv preprint arXiv:1903.02803, (2019).
- [6] C. CHEN, X. JIANG, W. CHEN, AND G. YAO, *Fast Solution for Solving the Modified Helmholtz Equation with the Method of Fundamental Solutions*, Communications in Computational Physics, 17 (2015), pp. 867–886.
- [7] G. FAIRWEATHER AND A. KARAGEORGHIS, *The method of fundamental solutions for elliptic boundary value problems*, Advances in Computational Mathematics, 9 (1998), p. 69.
- [8] C. HAFNER, *The Generalized Multipole technique for Computational Electromagnetics*, Artech House Boston, 1990.
- [9] C. HAFNER AND L. BOMHOLT, *The 3D Electrodynamical Wave Simulator-3D MMP Software and Users Guide*, 1995.
- [10] M. HASSELL AND F.-J. SAYAS, *Convolution Quadrature for Wave simulations*, in Numerical simulation in physics and engineering, Springer, 2016, pp. 71–159.
- [11] M. KATSURADA AND H. OKAMOTO, *The collocation points of the fundamental solution method for the potential problem*, Computers & Mathematics with Applications, 31 (1996), pp. 123–137.
- [12] J. LIN, C. CHEN, AND C.-S. LIU, *Fast solution of three-dimensional Modified Helmholtz equations by the Method of Fundamental Solutions*, Communications in Computational Physics, 20 (2016), pp. 512–533.
- [13] C. LUBICH, *Convolution Quadrature and Discretized Operational Calculus. I*, Numerische Mathematik, 52 (1988), pp. 129–145.
- [14] C. LUBICH, *Convolution Quadrature and Discretized Operational Calculus. II*, Numerische Mathematik, 52 (1988), pp. 413–425.
- [15] C. LUBICH AND A. OSTERMANN, *Runge-Kutta Methods for Parabolic Equations and Convolution Quadrature*, Mathematics of Computation, 60 (1993), pp. 105–131.
- [16] F.-J. SAYAS, *Retarded Potentials and Time Domain Boundary Integral Equations: A Road Map*, vol. 50, Springer, 2016.
- [17] G. WANNER AND E. HAIRER, *Solving ordinary differential equations II*, Springer Berlin Heidelberg, 1996.